Journal of Applied Polymer Science

Controllable Preparation of Uniform Polystyrene Nanospheres with Premix Membrane Emulsification

Zhendong Liu,[1] Yangcheng Lu,[1] Man Zhang,[2] Weiming Wan,[1] Guangsheng Luo[1]

[1]State Key Laboratory of Chemical Engineering, Department of Chemical Engineering, Tsinghua University, Beijing 100084, China
[2]College of Food Science and Nutritional Engineering, China Agricultural University, Beijing 100083, China
Correspondence to: Y. Lu (E-mail: luyc@tsinghua.edu.cn)

ABSTRACT: The expansion of polymer nanosphere applications requires facile and versatile preparation techniques. In this study, combining circled premix membrane emulsification and thermally initiated miniemulsion polymerization, we developed a new strategy for preparing uniform polystyrene nanospheres within a duration as short as 1 h. The size of the nanospheres, ranging from 40 to 120 nm, was dependent on the premix membrane emulsification cycle number, the transmembrane flow rate, and the membrane pore size; this was almost consistent with characterizations of droplet size evolution. The coefficient of variation, around 15%, indicated that the size distribution of the nanospheres was still narrow, even as the monomer-to-water ratio was as high as 0.2. This method may be competitive for further applications because of its high production efficiency and low system requirements. © 2012 Wiley Periodicals, Inc. J. Appl. Polym. Sci. 129: 1202–1211, 2013

KEYWORDS: emulsion polymerization; membranes; nanoparticles; nanowires and nanocrystals

Received 26 May 2012; accepted 1 October 2012; published online 27 November 2012
DOI: 10.1002/app.38662

INTRODUCTION

Polymer nanomaterials allow the generation of superior chemical and physical properties that are quite different from those of their bulky counterparts. Driven by the ever-increasing applications in various areas such as electronics,[1] photonics,[2] conducting materials,[3] sensors,[4] medicine, and biotechnology,[5] many efforts have been devoted to the generation of polymer materials with defined morphology and desired characteristics; these efforts have led the development of synthetic routes to polymer nanospheres, polymer nanocapsules, nanofibers, nanotubes, and so on.[6]

Of these various nanostructured polymers, polymer nanospheres are matrix particles with characteristic sizes ranging from several tenths of nanometers to a few hundred nanometers and whose entire mass is solid; molecules may be adsorbed at the sphere's surface or encapsulated within the particles.[7,8] The preparation techniques for polymer nanospheres can be classified into two categories: dispersion methods from polymers and polymerization methods from monomers.[7,9] Methods such as solvent evaporation, salting-out, nanoprecipitation, dialysis, and supercritical fluid technology can be used for the preparation of polymer nanospheres from polymers. The polymerization methods for polymer nanosphere preparation include conventional emulsion polymerization, miniemulsion polymerization, and microemulsion polymerization. Also, suspension polymerization for the preparation of polymer crystals and spheres has also been reported.[10,11]

Because most monomers and polymers have low solubility in water, polymerization methods can usually use water as a solvent; this endows them with better security and adaptability. In conventional emulsion polymerization, because monomers with slight water solubility diffuse from droplets to water, polymerization is carried out in water, and polymer nanospheres are built from the center to the surface. Because of this mechanism, conventional emulsion polymerization bears the conspicuous disadvantages of poor homogeneity and long duration. In microemulsion polymerization, polymer microspheres are formed in micelles with diameters from 10 to 100 nm; this process needs excessive auxiliary agents and meets with restrictions in product size. In contrast with microemulsion polymerization, miniemulsion polymerization uses metastable nanosized droplets as microreactors; this makes it an attractive technique for the adjustable preparation of polymer nanospheres through the manipulation of droplets.[12–14]

Miniemulsion preparation is the first step in miniemulsion polymerization. Conventionally, miniemulsion can be achieved by the so-called high-energy emulsification methods that use high-shear stirring, colloid mills, homogenizers, and

ultrasound.[15,16] Continuously over the last decade, new methods have been pursued to reduce the demand on mechanical energy input for miniemulsion preparation. From this point, methods with low energy input for generating miniemulsions have been proposed; these include the phase-inversion temperature method[17,18] and the spontaneous method based on the ouzo effect.[19] These methods might be energy effective for specific systems yet limited for use over a wide range of applications.

With the fast development of microfluidics in recent years, emulsion droplets of various sizes have successfully been prepared by membrane emulsification[20–22] and microchannel emulsification.[23,24] Membrane emulsification requires a much lower energy input compared with mechanical emulsification and ultrasound emulsification;[25,26] meanwhile, membrane emulsification is more feasible for large-scale production.

There are two types of membrane emulsification processes: cross-flow (or direct) membrane emulsification and premix membrane emulsification.[27] In the former process, the emulsion is formed by the pushing of the to-be-dispersed phase through a membrane into the cross-flowing continuous phase. Typically, the mean droplet size is 2–50 times larger than the mean pore size, depending on the choice of the membrane, the cross flow velocity, the ratio between the two phases, and the transmembrane pressure.[21] In contrast to cross-flow membrane emulsification, premix membrane emulsification generates a fine emulsion from an already-made coarse emulsion; this is then extruded or homogenized through the membrane pore under pressure. Compared with cross-flow membrane emulsification, premix membrane emulsification has a distinguishing feature that can be used to prepare emulsions with a much smaller mean droplet size than the mean pore size.

Since its advent in 1996, applications of premix membrane emulsification have shown its effectiveness in the preparation of single emulsions,[28,29] multiple emulsions,[30] gel microbeads[31] and polymer microspheres.[32] However, the preparation of polymer nanospheres with premix membrane emulsification has rarely been reported, with a few exceptions in which polylactide nanoparticles and chitosan nanospheres were prepared from polymers.[33–35]

Herein, we present a facile process for preparing polystyrene nanospheres with uniform droplet size from monomers with circled premix membrane emulsification. In contrast with published works regarding premix membrane emulsification in which pressure has commonly been used as the driving force, a pump-driven process was investigated in this study, as pumps are generally favored for transporting fluids in industrial applications. Meanwhile, the pump-driven process facilitated research under high flow rates, which may generate different scenarios compared with the low or medium flow rates commonly studied in pressure-driven processes. As for the membrane, in this study, a plate membrane made by stainless steel with a large porosity was used as a dispersion medium. Compared with the tubular-membrane-like Shirasu porous glass membrane widely investigated in the literature, the plate membrane we used was easily fabricated and had the potential advantage of facile scaling up.

In this process, miniemulsion-containing nanosized styrene (St) monomer droplets were first prepared by circled premix membrane emulsification, and then, the miniemulsion was polymerized by thermal initiation. On the basis of the merits of both the premix membrane emulsification and the miniemulsion polymerization, several advantages of this preparation method could be foreseen. First, uniform polymer nanospheres could be prepared as long as monomer droplets with a narrow size distribution could be generated by circled premix membrane emulsification. Second, the size of the nanospheres could easily be adjusted over a broad range through changes in the emulsification conditions. Finally, compared with other preparation techniques from monomers, the process combining premix membrane emulsification and miniemulsion polymerization could be rapid and easily operated and scaled up. In this study, we examined droplet generation in the circled premix membrane emulsification, determined the relationship between the droplet size and the size of the final nanospheres, and systematically investigated the changing of the polymer nanospheres size and its distribution with operating parameters, including the emulsification cycle number, the ratio between the monomer and water, the transmembrane flux, and the membrane pore size.

EXPERIMENTAL

Materials

St, 2,2′-azobisisobutyronitrile (AIBN), sodium dodecyl sulfate, poly(vinyl alcohol), sodium hydrate (NaOH), alcohol (CH_3CH_2OH), and sodium sulfate (Na_2SO_4) were analytical grade. St and AIBN were obtained from Sinopharm Chemical Reagent Co. (Beijing, China) and TongGuang Fine Chemicals Co. (Beijing, China), respectively. Divinylbenzene (DVB; 55%) was purchased from Aldrich (St. Louis, MO). The other chemicals were all from Beijing Chemical Works (Beijing, China). AIBN was recrystallized in alcohol. St and DVB were washed with 1 *M* NaOH three times, washed with water three times, and dried with Na_2SO_4. Furthermore, St and DVB were stripped with N_2 to remove dissolved O_2 for at least 1 h before use. Other materials were used as obtained.

Circled Premix Membrane Emulsification

Figure 1 shows the experimental layout for the circled premix membrane emulsification. It contained a cross-flow membrane emulsifier (CFME) and a premix membrane emulsifier (PME). Stainless steel (type 316 L) microfiltration membranes with 1 and 2 μm average pore sizes were used in our experiments [Figure 2 shows the scanning electron microscopy (SEM) photographs of the membranes]. In the CFME, the size of the continuous flow channel was $10 \times 0.5 \times 0.5$ mm^3. Both CFME and the PME had the same active membrane area of 2.5 mm^2.

A rough emulsion was first prepared with the CFME. The monomer (with the initiator AIBN at 1 wt % and the crosslinker DVB at 5 vol %) and water [with the surfactants and stabilizers sodium dodecyl sulfate (0.5 wt %), poly(vinyl alcohol) (0.5 wt %), and Na_2SO_4 (0.3 wt %] served as the dispersed phase and the continuous phase, respectively. In this process, droplets of monomer were generated and dispersed in the water phase by shear force, which is an energy-efficient and

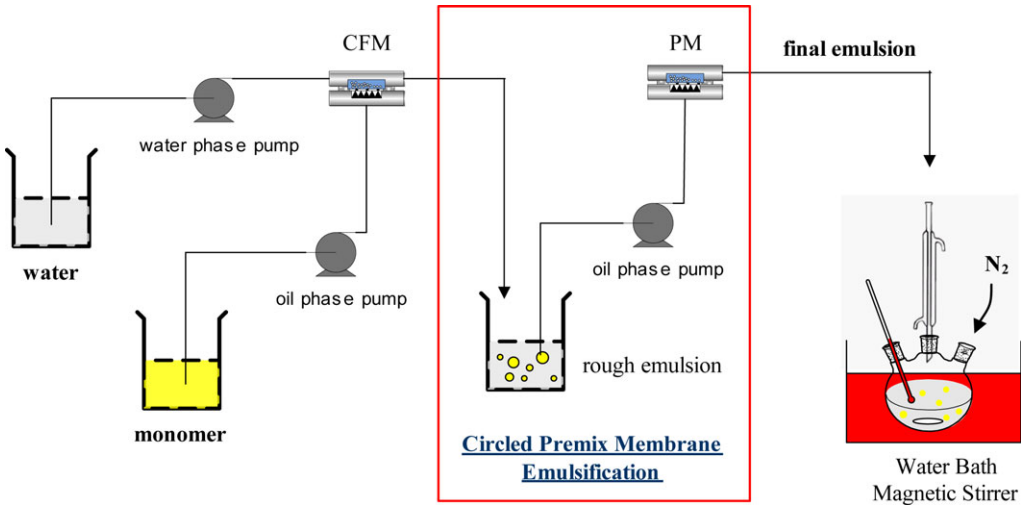

Figure 1. Experimental layout for the circled premix membrane emulsification. CFM, cross-flow module; PM, premix module. [Color figure can be viewed in the online issue, which is available at www.interscience.wiley.com.]

highly reproducible emulsification method.[25,26] Subsequently, the rough emulsion was pumped to pass the PME, where the size of the monomer droplets was decreased further under the function of hydrodynamic focusing when the two fluids simultaneously passed through the membrane pores. The product emulsion was used for polymerization or pumped to pass the PME again. The time that the PME was used is denoted as the cycle number.

Preparation of the Polymer Nanospheres

Polymerization was carried out in a three-necked flask immersed in an oil bath controlled at 85 °C. Typically, 30 mL of emulsion was added to a 50-mL flask and stirred at 1000 rpm with a magnetic stirrer. All of the polymerization reactions were carried out under persistent nitrogen protection. A condenser pipe was used to prevent evaporation during polymerization. After a certain reaction time, the polymerized emulsion was cooled by an ice bath and demulsified by the addition of alcohol. Finally, the polymer nanospheres were collected and washed three times with deionized water.

Analysis

Laser scattering, which was carried out with a Malvern Mastersizer 2000 (Malvern Instruments, Malvern, United Kingdom), was used to analyze the droplet size in the emulsions. Each sample was analyzed in triplicate. The droplet size of the miniemulsion was described by the number-average droplet size ($d_{d,av}$).The droplet size distribution was characterized by a coefficient of variation (CV). The two variables are defined as follows:

$$d_{d,av} = \frac{\sum_{i=1}^{N} d_{d,i}}{N}$$

$$CV = \frac{(\sum_{i=1}^{N} (d_{d,i} - d_{d,av})^2 / N)^{\frac{1}{2}}}{d_{d,av}}$$

where $d_{d,i}$ is the diameter of the ith droplet and N is the total number of droplets observed.

The morphology of the polymer nanospheres was characterized by SEM (JSM 7401 F, JEOL, Tokyo, Japan) and transmission

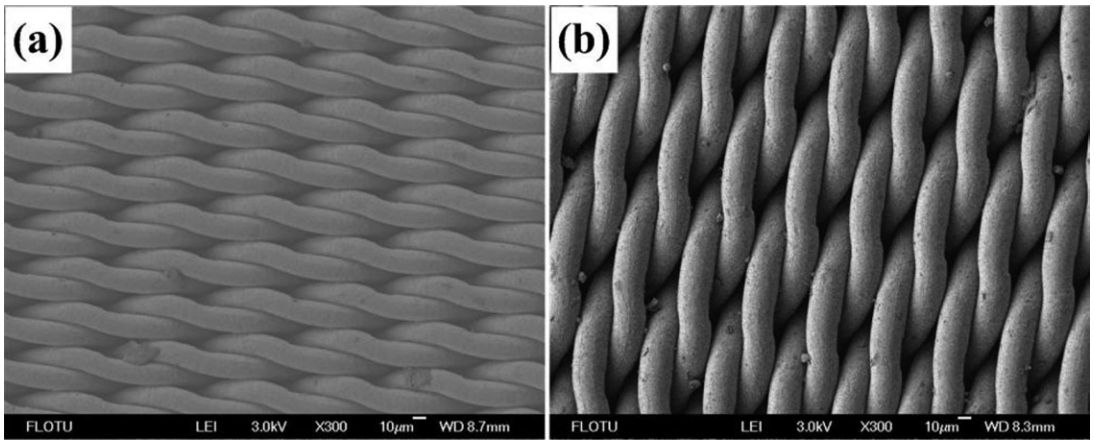

Figure 2. SEM photographs of the stainless steel microfiltration membranes: average pore sizes of (a) 1 and (b) 2 μm.

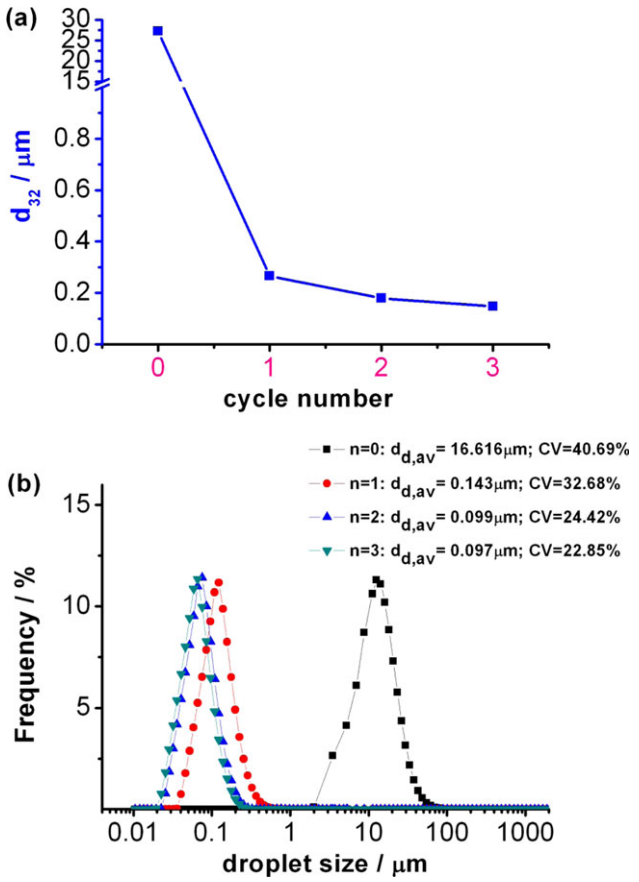

Figure 3. Variation of the droplet size and its distribution with emulsification cycle. The experimental conditions were as follows: 1 mL/min for the monomer phase and 20 mL/min for the water phase in CFME and 20 mL/min in PME and with a membrane with pore size of 1 μm. n is the count of the emulsion passing through the premix module. [Color figure can be viewed in the online issue, which is available at www.interscience.wiley.com.]

electron microscopy (TEM; JEM 2010, JEOL, Tokyo, Japan). The size of the nanospheres and its distribution were determined by the processing of TEM photographs. The number of spheres observed for the size analysis was above 200 for each sample to ensure accuracy. The mean size and size distribution of the nanospheres were also represented by the number-average diameter ($d_{p,av}$) and CV, respectively.

RESULTS AND DISCUSSION

Droplet Generation

It has generally been observed that for cross-flow membrane emulsification, the ratio of the droplet diameter to the pore diameter typically ranges from 2 to 10, depending on the membrane materials and operational conditions.[21] However, premix membrane emulsification can easily produce droplets with sizes smaller than membrane pore size. As shown in the experimental results in Figure 3(a), the average droplet size (d_{32}) decreased sharply from 27.257 μm after cycle number 0 (cross-flow membrane emulsification only) to 0.266 μm after cycle number 1 (first cycle of premix membrane emulsification). Evidently, the average droplets size obtained after premix membrane emulsification was smaller than the mean membrane pore size (1 μm).

Compared with droplet generation in cross-flow membrane emulsification, in which the droplet detaches from the membrane pore because of the shear stress of the continuous flow, droplet breakup in premix membrane emulsification is much more complicated and, hence, not very clear so far. van der Zwan et al.[36] used microchannels as simulated membrane pores to microscopically visualize droplet breakup in premix membrane emulsification. They found that three droplet breakup mechanisms existed in premix membrane emulsification: snap off due to localized shear forces, breakup due to interfacial tension effects (including Laplace instability and Rayleigh instability), and breakup due to steric hindrance between droplets. However, the flow rates in their research were relatively low, mostly because of the convenience of using the visualization method, and therefore, the final droplet size was still larger than the size of the microchannel pore. In practice, premix membrane emulsification is generally operated at high flow rates (or high pressure) to further decrease the droplet size. Actually, droplets with sizes smaller than the membrane pore size appeared only if the operational flow rates or driving pressure was enough high. This fact implies that van der Zwan's work might not cover all droplet breakup mechanisms in premix membrane emulsification, and other mechanisms may exist that result in smaller droplets at a different operational conditions.

According to the flow state, the droplet breakup mechanism in membrane emulsification could be classified into two categories: laminar breakup mechanism[37] and turbulent breakup mechanism.[38] Under laminar flow, the droplet first deforms into a cylindrical liquid thread under shear stress, and then, when the length of the cylindrical liquid thread exceeds its circumstance, it breaks into smaller droplets on the basis of Rayleigh–Plateau instability.[39] In a turbulent regime, droplet breakup occurs because of the fact that the turbulent stress exerted on the droplet surface exceeds the interfacial force maintaining the droplet uniformity. Depending on the relationship between the droplet size and the length of the Kolmogorov energy dissipating eddy, droplet breakup in the turbulent state can be further caused by two mechanisms:[38,40] the inertial breakup mechanism, which occurs when the size of the droplet is larger than the length of the turbulent eddy, and viscous breakup mechanism, which occurs when the size of the droplet is smaller than the length of the turbulent eddy. In the laminar regime, droplets with a size equal to the membrane pore size could be generated, yet a further decrease in the droplet size in large proportion was not possible (smaller satellite droplets could be generated because of local pressure fluctuations but in a limited number). On the contrary, the mass generation of droplets whose size is smaller than the membrane pore size could be realized in a turbulent regime because the turbulence is extensive and the length of the Kolmogorov energy dissipating eddy generated in the flow is small enough.

On the basis of previous theories, a mechanism of droplet generation mechanism is proposed in this article. Under the operational conditions in this study, turbulence could be very easily generated because of the high velocities of both phases and complicated passage geometry, as membrane walls posed as obstacles. So, before and after the membrane pore, the flow state was turbulent, whereas inside the membrane pore, because of the dominant surficial effect, the flow was exactly laminar.

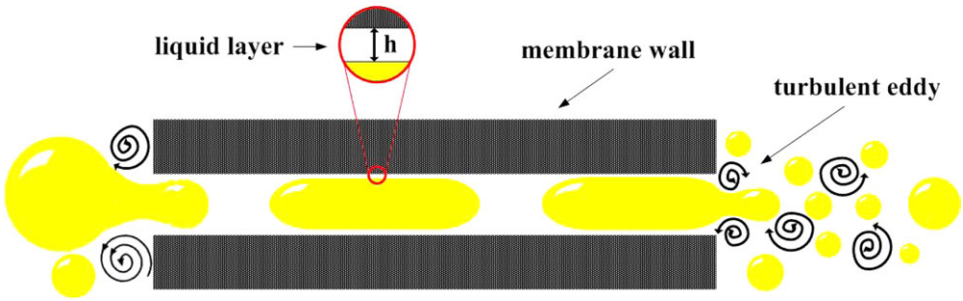

Figure 4. Illustration of the droplet breakup mechanism in the premix membrane emulsification. [Color figure can be viewed in the online issue, which is available at www.interscience.wiley.com.]

Thus, as shown in Figure 4, before the membrane pore, the parent droplet from the last stage of emulsification deformed and entered the membrane pore under pressure, where it may or may not have broken into small droplets whose size was still larger than the pore size. While flowing in the membrane pore, the droplet was stretched into a cylindrical thread under wall shear stress, and between the thread and the membrane wall, a liquid layer presented, whose thickness was dependent on the operational conditions, such as the flow rates, membrane pore size, and system properties, such as viscosity and interfacial force.[41] Immediately after the membrane pore, where extensive turbulence was generated because of the effect of the suddenly enlarged flow passage, the stretched cylindrical thread was broken into smaller droplets by turbulent eddies. The size of daughter droplets was dependent on the turbulence level. If the turbulence was extensive and the size of the eddies generated was smaller than that of the membrane pore, the generation of droplets with a mean size much smaller than the mean membrane pore size was possible. In brief, it was the combined function of the stretching effect inside the membrane pore and the turbulent eddies in the immediate outlet of the membrane pore that forced the parent droplet broken into daughter droplets with a mean size smaller than the mean membrane pore size.

As shown in Figure 3(b), almost all of the droplets generated by cross-flow membrane emulsification were much larger than the membrane pore size. After the first premix membrane emulsification cycle, the droplet size experienced a sharp reduction, but big droplets still existed in the emulsion as indicated by the broader droplet size distribution. We speculated that although droplets with a size smaller than the pore size were generated under a turbulent breakup mechanism, droplets with a bigger size still existed, partly because of the fact that the generation of smaller droplets also depended on probability. When this emulsion was recirculated to pass through the membrane again, more large droplets were broken into smaller ones, and thus, the mean droplet size decreased when homogeneity was improved. In the third cycle, the decrease in the droplet size was not so conspicuous; this indicated that the turbulence could not decrease the droplet size further. In the meanwhile, the homogeneity of the droplet size was only slightly improved; this possibly corresponded to a balance of droplet coalescence and breakup.

Morphology and Generation Mechanism of the Polymer Nanospheres

Figure 5 shows the typical SEM and TEM photographs of the polymer nanospheres after 1 h of polymerization; these confirmed that polymer nanospheres with uniform sizes were successfully prepared with circled premix membrane emulsification combined with miniemulsion polymerization. Also, the nanospheres were perfect spheres with a very smooth surface and were well dispersed without the formation of aggregates. In

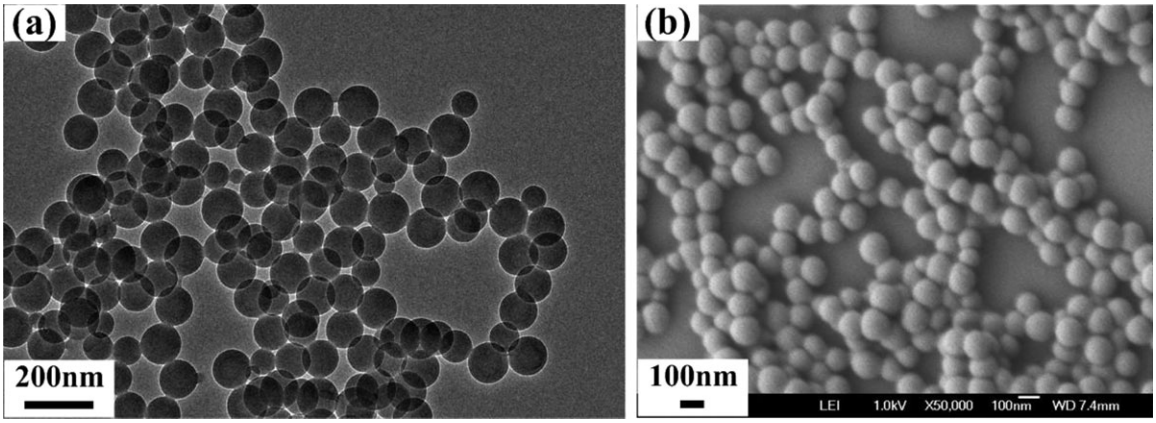

Figure 5. TEM and SEM photographs of the polymer nanospheres. The experimental conditions were as follows: 1 mL/min for the monomer phase and 20 mL/min for the water phase in CFME and 20 mL/min in PME, with a membrane with a pore size of 1 μm, cycle number of 1, and polymerization time of 1 h.

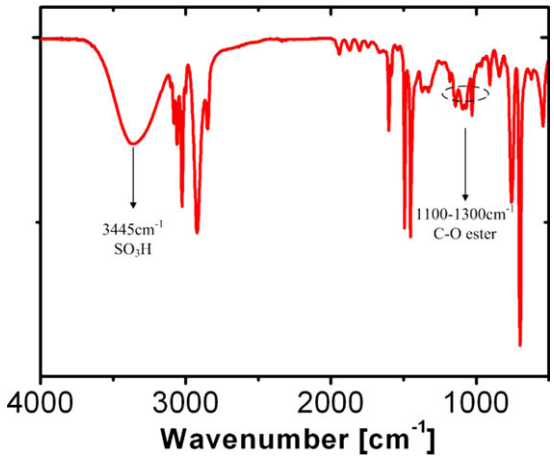

Figure 6. Representative Fourier transform infrared spectrum of the polymer nanospheres. The spectrum clearly indicates the presence of the stretching frequencies of all of the monomers. Also, the signals at 3445 and 1100–1300 cm^{-1} showed the presence of residual surfactants on the surface of the nanospheres. [Color figure can be viewed in the online issue, which is available at www.interscience.wiley.com.]

our preliminary experiments, we found that the miniemulsion polymerization required a duration long enough to make product performance good in morphology and monodispersity. When the polymerization time was 40 min or shorter, the polymer particles aggregated together and showed irregular shapes; this was related to a lower conversion of monomers (ca. 75% conversion for 40 min). However, the polymerization time could be set at 1 h (approximate total conversion) to ensure that polystyrene nanospheres with good morphology were prepared in this study. The phenomenon that incomplete conversion of a monomer could lead to nonspherical polymer particles without smooth surfaces was also observed in another work.[42]

Figure 6 shows the representative Fourier transform infrared spectrum of the polymer nanospheres. The spectrum clearly indicates the presence of stretching frequencies for all of the monomers (St and DVB), and therefore, we concluded from this figure that the polymer nanospheres synthesized by this method were made up of the poly(styrene-*co*-divinylbenzene) structure. Meanwhile, signals at 3445 cm^{-1} (contributed to the stretching vibrations of the SO_3H bond) and 1100–1300 cm^{-1} (contributed to the stretching vibrations of the C—O ester bond) were also observed in this spectrum. This indicated the presence of residual surfactants on the surface of the nanospheres because the surfactants were very difficult to totally remove from the nanospheres.

Figure 7 shows the representative size distributions of the monomer droplets before polymerization and the corresponding polymer nanospheres. Conspicuous shrinkage from the monomer droplets to the polymer nanospheres was observed: the average size of the polymer nanospheres was about 30% smaller than that of the monomer droplets. This size difference between droplets and nanospheres could be interpreted from two reasons. For one thing, because of the density difference between the polymer and the monomer, the size of polymer spheres could be smaller than that of monomer droplets. For another, as a surfactant and stabilizer were used in the experiments, the monomer droplets were covered by molecules with long chains, which may have increased the measurement error of laser scattering characterization. Moreover, the resolution of the size measurement equipment may have also caused results in which the droplet size distribution was broader than the nanosphere size distribution, as pointed by Yanagishita et al.,[43] who had similar experimental results.

Evidently, the size distribution of nanospheres, which seems dependent on the size distribution of microdroplets directly, can be predicted or controlled on the basis of the rules that the premix membrane emulsification obeys, although the coalescence of monomer droplets cannot be totally avoided.

Controllability of the Preparation Method

Effect of the Cycle Number. The effect of the premix membrane emulsification cycle number on the size and uniformity of the polymer nanospheres was investigated. Figure 8(a–c) shows the typical morphologies of polymer nanospheres obtained after different emulsification cycles from 1 to 3. Figure 8(d) shows the trends of the mean sphere size and its CV. Cycle 0, in which premix membrane emulsification did not work, was not included because, in that case, the droplet size was larger than 10 μm and was not applicable for stable polymerization.

We observed that the size of the polymer nanospheres decreased with the emulsification cycle number. A conspicuous difference in the nanosphere size was observed between cycles 1 and 2, although there was only a slight decrease in size from cycle 2 to cycle 3. As for the uniformity of polymer nanospheres, an increase in the emulsification cycle number improved the homogeneity of the nanospheres slightly. This trend was in good accordance with the droplet size changes with cycle number, as shown in Figure 3(b). Thus, the effect of the premix membrane emulsification cycle number on the size and uniformity of the polymer nanospheres could be interpreted from the changes in the droplet: with increasing emulsification cycle number, the chance that bigger droplets were broken into smaller ones under turbulence increased, so the mean droplet size decreased, and the uniformity

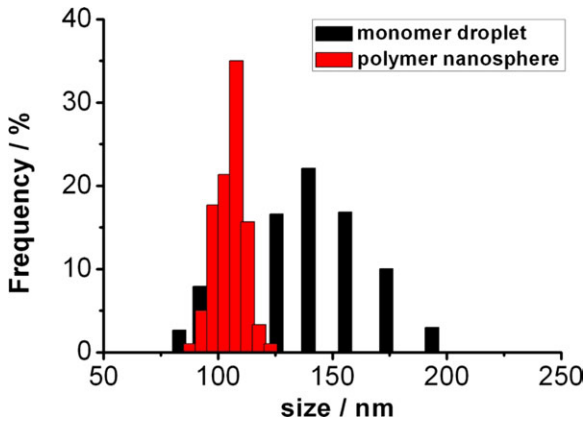

Figure 7. Size distributions of the monomer droplets in the emulsions and polymer nanospheres. The experimental conditions were all the same as shown in Figure 5. [Color figure can be viewed in the online issue, which is available at www.interscience.wiley.com.]

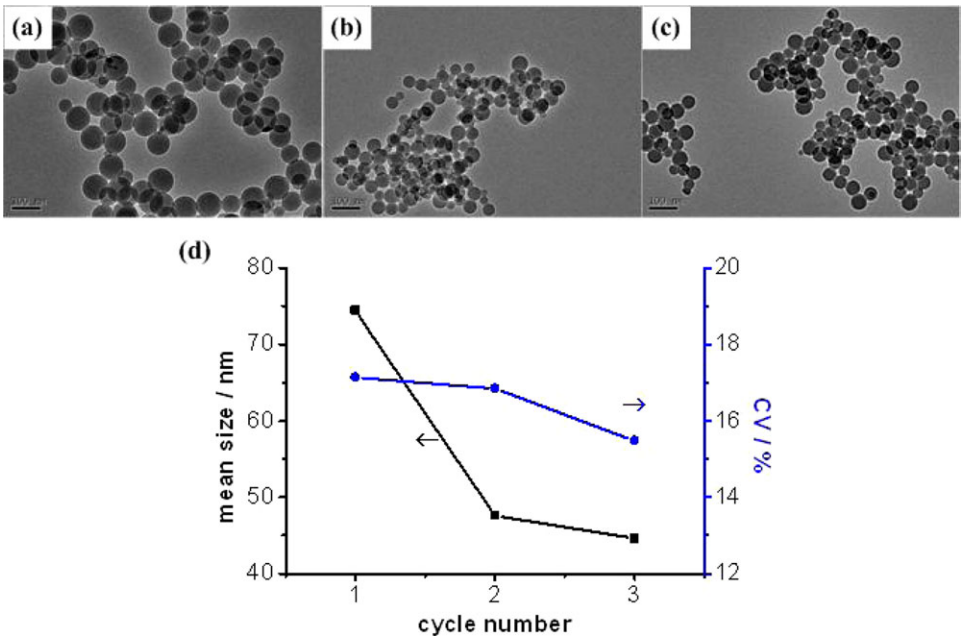

Figure 8. Effect of the emulsification cycle number on the size of the polymer nanospheres and its distribution. The experimental conditions were as follows: 1 mL/min for the monomer phase and 20 mL/min for the water phase in CFME and 20 mL/min for PME, with a membrane with an average pore size of 1 μm and a polymerization time of 1 h. [Color figure can be viewed in the online issue, which is available at www.interscience.wiley.com.]

of the droplet size was further improved as well. After the second premix membrane emulsification cycle, the size of the droplets reached a considerably small level; this implied that it could be more difficult for turbulent eddies to cause droplet breakup. Also, the probability of the generation of smaller droplets under the same operating conditions decreased sharply. Apparently, by combining circled premix membrane emulsification with miniemulsion polymerization, we could adjusted the size of the polymer nanospheres through changing the emulsification cycle. Meanwhile, the size uniformity was always under control.

Effect of the Monomer-to-Water Ratio. The flow rate of the monomer in CFME was changed singly to study the effect of the monomer-to-water ratio. Figure 9 gives the results. As shown, the increase in the monomer phase fraction led to an increase in the size of the polymer nanospheres; this indicated that increasing the monomer-to-water ratio could result in emulsions with bigger droplets.

From the first observation, an increase in the oil-phase flow in the cross-flow membrane emulsification generated a coarse emulsion with bigger droplets. However, previous studies showed that the droplet size in coarse emulsions did not significantly affect the droplet size after premix membrane emulsification, so inefficiency in the cross-flow membrane may not have been the decisive reason for the droplet increase. Consider the expression of the length of the Kolmogorov energy dissipating eddy:[38,40]

$$l_K = \left(\frac{\eta_e}{\rho_e}\right)^{3/4} \frac{1}{\varepsilon^{1/4}} \quad (1)$$

where lk, length of Kolmogorov energy dissipating eddies; ηe, viscosity of the emulsion; ηE, extensional viscosity of fluid; ρ, total specific power dissipation;pe, density of the emulsion.

We found that the length of the turbulent eddy increased because the emulsion viscosity increased and the emulsion density decreased with increasing monomer-to-water ratio. Accordingly, a decreased turbulent level generated fine emulsions with bigger droplets. As for the uniformity of the polymer nanospheres, we observed that the CV did not change apparently with the monomer-to-water ratio; this probably indicated that after three cycles of premix membrane emulsification, the uniformity of the droplets approached its optimal value.

Effect of the Transmembrane Flow Rate. The flow rate in PME was changed solely to study the effect of the transmembrane flow rate. Similar to the previous results, Figure 10(a–c) shows typical TEM photographs of the polymer nanospheres, and Figure 10(d) shows the changes in the mean size and CV with various transmembrane flow rates.

As stated in the discussion of droplet generation, two functions, the stretching effect inside the membrane pore and the turbulent breakup immediately outside the pore, facilitated droplet generation in the premix membrane emulsification. On the one hand, high flow rates were favored for extensive turbulence; on the other hand, high flow rates could have also helped in stretching the to-be-dispersed phase because the liquid layer between the membrane wall surface and the stretched thread increased with flow rate, as governed by following expression:[41]

$$h \propto R_p \left(\frac{\eta_e Q}{\gamma}\right)^{2/3} \quad (2)$$

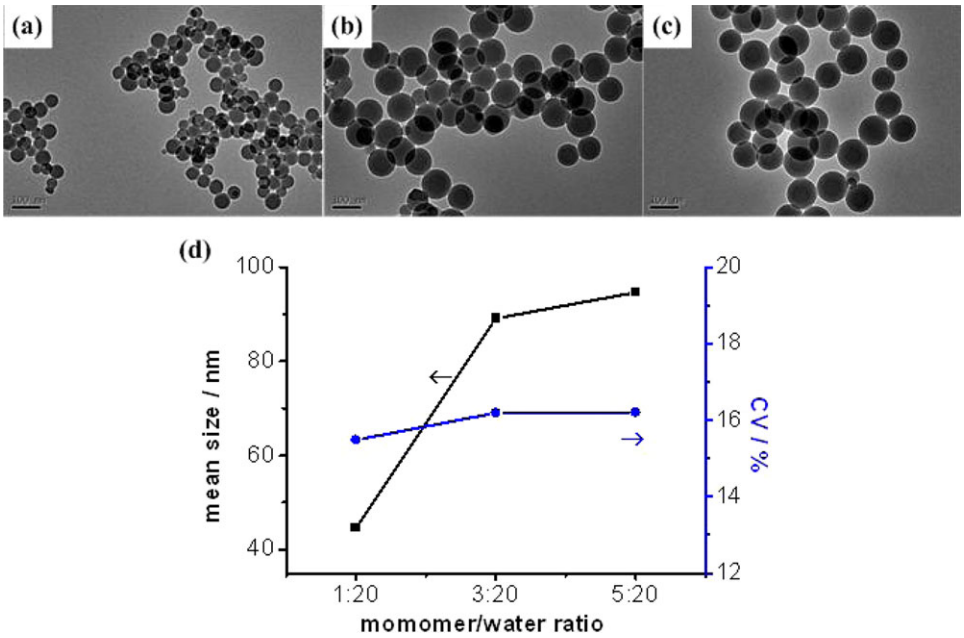

Figure 9. Effect of the monomer-to-water ratio on the size of the polymer nanospheres and their distribution. The experimental conditions were as follows: 1, 3, and 5 mL/min (from left to right) for the monomer phase and 20 mL/min for the water phase in CFEM and 20 mL/min for PME, emulsification cycle three, with a membrane with an average pore size of 1 μm and a polymerization time of 1 h. [Color figure can be viewed in the online issue, which is available at www.interscience.wiley.com.]

where Q, flow rate; r, the surface tension; Rp, the radius of the pore (on the membrane in this work); h, the thickness of liquid layer between the pore wall and the dispersed fluid; ηe, viscosity of the emulsion.

Clearly, with increasing flow rates, the size of the nanospheres decreased, as the parent droplet inside the membrane pore was more stretched and the turbulent force increased with the transmembrane flow rates. This, thereby, enabled the generation of

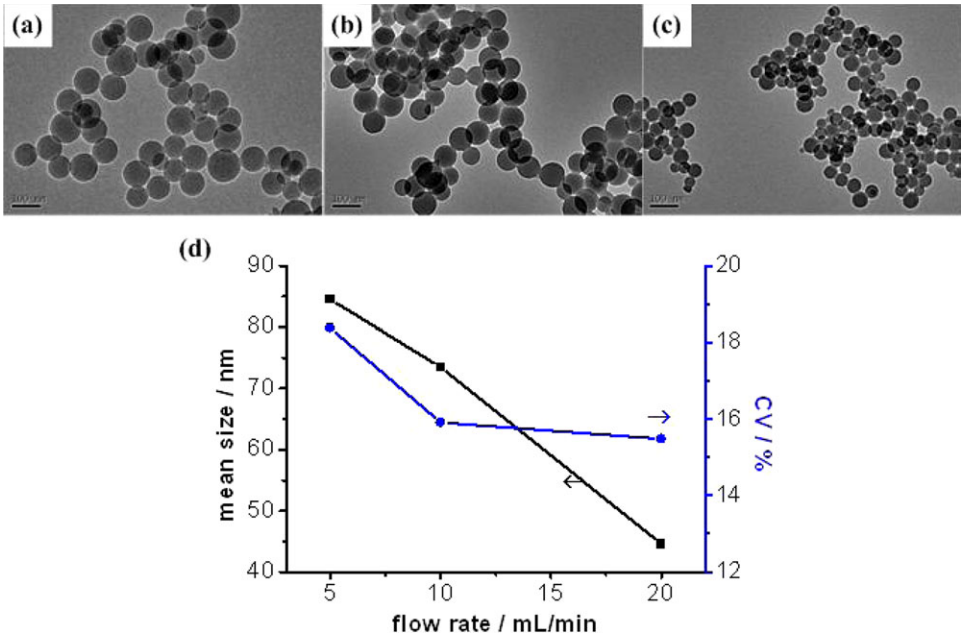

Figure 10. Effect of the transmembrane flow rates on the size of the polymer nanospheres and their distribution. The experimental conditions were as follows: 1 mL/min for the monomer phase and 20 mL/min for the water phase in CFME, 5, 10, and 20 mL/min (from left to right) for PME, emulsification cycle three, with a membrane with an average pore size of 1 μm and a polymerization time of 1 h. [Color figure can be viewed in the online issue, which is available at www.interscience.wiley.com.]

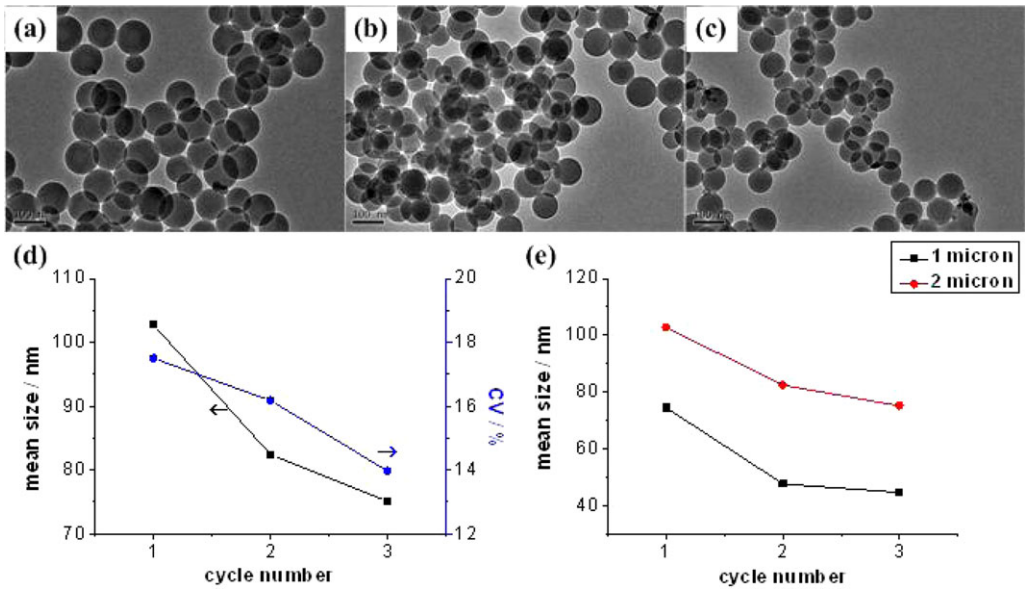

Figure 11. Characterizations of the nanospheres prepared with 2 -μm membranes. The experimental conditions were as follows: 1 mL/min for the monomer phase and 20 mL/min for the water phase in CFME, 20 mL/min for PME, with a membrane with an average pore size of 2 μm and a polymerization time of 1 h. [Color figure can be viewed in the online issue, which is available at www.interscience.wiley.com.]

smaller droplets in the product emulsion. From the comparison of CV values, we observed that with increasing transmembrane flow rate, the uniformity of the polymer nanospheres was improved. From the viewpoint of probability, it was obvious that a higher number of cycles of premix membrane emulsification were needed to approach optimal homogeneity because the transmembrane flow rate was low (e.g., 5 mL/min).

Effect of the Membrane Pore Size. To investigate the effect of the membrane pore size in the preparation of the polymer nanospheres with circled premix membrane emulsification, another membrane with a mean pore size of 2 μm was used for comparison. The results are shown in Figure 11. From this figure, it can be seen that the minimum size of the nanospheres was about 80 nm, approximately two times the size of the nanospheres obtained with 1 -μm membranes under the same operational conditions. Meanwhile, the uniformity of the nanospheres obtained with 2 -μm membranes stayed at the same level as that obtained with 1 -μm membranes [shown in Figure 8(d)]. From this comparison, we concluded that the membrane pore size influenced the size of the final nanospheres but had no apparent effect on the size distribution of the nanospheres, so changing the membrane pore size is another choice for adjusting the sizes of polymer nanospheres.

CONCLUSIONS

In this study, with a combination of circled premix membrane emulsification and miniemulsion polymerization, uniform polystyrene nanospheres were successfully prepared. The size of the nanospheres could be controlled from 40 to 120 nm. The size distribution of the nanospheres was very narrow with an optimal CV of about 13%. The reaction time was about 1 h, which was much shorter than that of conventional methods such as emulsion polymerization.

This method included two steps: miniemulsion preparation with circled premix membrane emulsification and miniemulsion polymerization by thermal initiation. Because the polymer nanospheres were copies of the droplets in miniemulsion, the size distribution of the nanospheres could be predicted or controlled on the basis of rules that the premix membrane emulsification obeyed.

The parameters that influenced the size of polymer nanospheres and its uniformity were investigated, with following conclusions found: (1) increasing the emulsification cycle decreased the size of nanospheres and improved their uniformity; (2) as the cycle number for premix membrane emulsification was constant, decreasing the monomer-to-water ratio or transmembrane flow rate decreased the size of the nanospheres and narrowed the size distribution; and (3) for certain operational conditions, the size of the polymer nanospheres depended on the membrane pore size, but the membrane pore size had little influence on the uniformity of the nanospheres.

In general, the combination of circled premix membrane emulsification and miniemulsion polymerization is a facile and versatile method for preparing uniform polymer nanospheres with controllable sizes. However, the droplets evolving mechanism in the circled premix membrane emulsification process needs more research as the fundamentals of this method.

ACKNOWLEDGMENT

The authors gratefully acknowledge the support of the National Natural Science Foundation of China (contract grant numbers

20525622, 20876084, and 21036002) and the National Basic Research Program of China (contract grant number 2007CB714302).

REFERENCES

1. Andres, C. A.; Samori, P. *Nat. Chem.* **2011**, *3*, 431.
2. Fudouzi, H.; Xia, Y. *Adv. Mater.* **2003**, *15*, 892.
3. Luo, S. C.; Zhu, B.; Nakao, A.; Nakatomi, R.; Yu, H. H. *Adv. Eng. Mater.* **2011**, *10*, B423.
4. Brahim, S.; Narinesingh, D.; Elie, G. A. *Anal. Chim. Acta* **2001**, *448*, 27.
5. Zhang, L. J.; Webster, T. J. *J. Biomed. Mater. Res. A* **2012**, *1*, 94.
6. Yoon, H.; Choi, M.; Lee, K. J.; Jiang, J. *Macromol. Res.* **2008**, *2*, 85.
7. Rao, J. P.; Geckeler, K. E. *Prog. Polym. Sci.* **2011**, *36*, 887.
8. Vauthier, C.; Couvreur, P. In Handbook of Pharmaceutical Controlled Release Technology; Wise, D. L., Ed.; Marcel Dekker: New York, **2000**; p 413.
9. Vauthier, C.; Bouchemal, K. *Pharm. Res.* **2008**, *5*, 1025.
10. Okubo, T. *Prog. Polym. Sci.* **1993**, *3*, 481.
11. Okubo, T. *Langmuir* **1994**, *10*, 1695.
12. Antonietti, M.; Landfester, K. *Prog. Polym. Sci.* **2002**, *27*, 689.
13. Landfester, K. *Angew. Chem. Int. Ed.* **2009**, *48*, 4488.
14. Hu, J.; Chen, M.; Wu, L. *Polym. Chem.* **2011**, *2*, 760.
15. Solans, C.; Izquierdo, P.; Nolla, J.; Azemar, N.; Garcia-Celma, M. *J. Curr. Opin. Colloid Interface Sci.* **2005**, *10*, 102.
16. Karbstein, H.; Schubert, H. *Chem. Eng. Process.* **1995**, *34*, 205.
17. Rang, M. J.; Miller, C. A. *J. Colloid Interface Sci.* **1999**, *209*, 179.
18. Izquierdo, P.; Esquena, J.; Tadros, T. F.; Dederen, J. C.; Feng, J.; Garcia-Gelma, M. J.; Azemar, N.; Solans, C. *Langmuir* **2004**, *20*, 6594.
19. Ganachaud, F.; Katz, J. L. *Chem. Phys. Chem.* **2005**, *6*, 209.
20. Vladisavljević, G. T.; Williams, R. A. *Adv. Colloid Interface Sci.* **2005**, *113*, 1.
21. Charcosset, C.; Limayem, I.; Fessi, H. *J. Chem. Technol. Biotechnol.* **2004**, *79*, 209.
22. Joscelyne, S. M.; Trägårdh, G. *J. Membr. Sci.* **2000**, *169*, 107.
23. Sugiura, S.; Nakajima, M.; Seki, M. *Langmuir* **2002**, *18*, 5708.
24. Sugiura, S.; Nakajima, M.; Seki, M. *Ind. Eng. Chem. Res.* **2004**, *43*, 8233.
25. Lambrich, U.; Schubert, H. *J. Membr. Sci.* **2005**, *257*, 76.
26. Schuber, H.; Engel, R. *Chem. Eng. Res. Des.* **2009**, *82*, 1137.
27. Nazir, A.; Schroën, K.; Boom, R. *J. Membr. Sci.* **2010**, *362*, 1.
28. Trentin, A.; De Lamo, S.; Güell, C.; López, F.; Ferrando, M. *J. Food. Eng.* **2011**, *106*, 267.
29. Trentin, A.; Güell, C.; López, F.; Ferrando, M. *J. Membr. Sci.* **2010**, *356*, 22.
30. Vladisavljević, G. T.; Shimizu, M.; Nakashima, T. *J. Membr. Sci.* **2004**, *244*, 97.
31. Zhou, Q. Z.; Wang, L. Y.; Ma, G. H.; Su, Z. G. *J. Colloid Interface Sci.* **2007**, *311*, 118.
32. Yang, J.; Hao, D. X.; Bi, C. X.; Su, Z. G.; Wang, L. Y.; Ma, G. H. *Ind. Eng. Chem. Res.* **2019**, *49*, 6047.
33. Sawalha, H.; Purwanti, N.; Rinzema, A.; Schroën, K.; Boom, R. *J. Membr. Sci.* **2008**, *310*, 484.
34. Wei, Q.; Wei, W.; Lai, B.; Wang, L. Y.; Wang, Y. X.; Su, Z. G.; Ma, G. H. *Int. J. Pharm.* **2008**, *359*, 294.
35. Lv, P. P.; Wei, W.; Gong, F. L.; Zhang, Y. L.; Zhao, H. Y.; Lei, J. D.; Wang, L. Y.; Ma, G. H. *Ind. Eng. Chem. Res.* **2009**, *48*, 8819.
36. van der Zwan, E.; Schroën, K.; van Dijke, K.; Boom, R. *Colloid Surf. A* **2006**, *277*, 223.
37. Fischer, P.; Erni, P. *Curr. Opin. Colloid Interface Sci.* **2007**, *12*, 196.
38. Boxall, J. A.; Koh, C. A.; Sloan, E. D.; Sum, A. K.; Wu, D. T. *Langmuir* **2012**, *28*, 104.
39. Saeki, D.; Sugiura, S.; Kanamori, T.; Sato, S.; Mukataka, S.; Ichikawa, S. *Langmuir* **2008**, *24*, 13809.
40. Almeida-Rivera, C.; Bongers, P.; *Comput. Chem. Eng.* **2012**, *37*, 33.
41. Hunter, D. G.; Frisken, B. *J. Biophys. J.* **1998**, *74*, 2996.
42. Su, G.; Mogi, T.; Konno, M. *J. Colloid Interface Sci.* **1998**, *207*, 113.
43. Yanagishita, T.; Fujimura, R.; Nishio, K.; Masuda, H. *Langmuir* **2010**, *3*, 1516.